applied optics

Antitwilight I: structure and optics

DAVID K. LYNCH,[1,*] DAVID S. P. DEARBORN,[2] AND STEVEN C. RICHTSMEIER[3]

[1]*Thule Scientific, P.O. Box 953, Topanga, California 90290, USA*
[2]*Lawrence Livermore National Laboratory, 7000 East Ave, Livermore, California 94550, USA*
[3]*Spectral Sciences, Inc. 4 Fourth Ave., Burlington, Massachusetts 01803-3304, USA*
Corresponding author: david@alumni.caltech.edu

Time-lapse videos, still photos, visual observations, and theoretical studies were used to investigate the antitwilight, i.e., twilight opposite the Sun. Colors, brightnesses, and antitwilight features as a function of solar altitude were measured. Four roughly horizontal bands were identified and explained physically in terms of atmospheric geometry, the observer's line-of-sight, optical depth, refraction, and multiple scattering. Particular emphasis is placed on (1) the origin of the dark segment, (2) the rapid rising of the Belt of Venus with solar altitude, and (3) ray tracing light through the low atmosphere to understand refractive effects. New names are suggested for three of the four bands, and the new terminology is reconciled with earlier papers.   © 2017 Optical Society of America

OCIS codes: (000.4930) Other topics of general interest; (010.0010) Atmospheric and oceanic optics; (080.0080) Geometric optics.

https://doi.org/10.1364/AO.56.00G156

1. INTRODUCTION

Twilight is sunlight scattered by the atmosphere that is visible when the Sun is below the horizon [1,2]. Specifically, it is sunlight that has been refracted and singly or multiply scattered by the atmosphere, and visible to an observer when the refracted Sun is below his refracted horizon. Twilight occurs when the Sun is in the altitude range −18° to 0°, though if the atmosphere is very turbid, it can be seen for solar altitudes of −23° [2]. Twilight colors are enormously complex and their brightnesses change by factors of 10^5–10^6 in about an hour in the tropics, longer at mid and high latitudes. Add to this the highly variable aerosol loading of the atmosphere and the speed with which antitwilight changes, and it is difficult to assemble a generalized yet quantitative description of twilight. Perhaps this is the reason that even today, visual characterizations of twilight remain qualitative and often ambiguous. Many references summarize visual aspects of twilight [3–6], but the terminology is often so inconsistent that it is sometimes hard to know exactly what the authors are talking about.

In order to place antitwilight phenomenology on a more uniform, quantitative basis, we undertook a series of observations with no expectation other than to take a fresh look at antitwilight and capture it digitally for further analysis. We quickly noticed several phenomena that, while consistent with previous reports, had not been explicitly described and explained. These led to the present paper. Here our goals are to (1) present a unified, observation-based description of the antisolar twilight ("antitwilight"), (2) explain the physical basis for its various components, (3) reveal the reason for the rapid movement of the Belt of Venus compared to the solar altitude

change [3,7], and (4) explain the dark segment, in which the "shadow of the Earth" paradoxically seems to be visible when the Sun is above the horizon [8]. Sections 2–4 present observational results only, with no physical interpretation. Sections 5–7 explain the physical basis for the observations, and Section 8 discusses the dark segment. For clarity we use the term "altitude" to denote angle in the sky relative to the horizon and "elevation" to refer to vertical distance (km) above sea level.

2. VISUAL OBSERVATIONS

Our first approach was to simply observe the antisolar twilight by eye while looking over the ocean, the darkest and simplest landscape. The fact that color can be seen during all phases of twilight means that visual detection is via photopic or mesopic vision. To our surprise, the time progression of colors, positions, and brightnesses were the same regardless of the surrounding landscape illumination, provided that the sky was clear and cloud free. Observations made looking west over Santa Monica Bay at the morning antitwilight with the blazing lights of Los Angeles to the east were identical to those observed from Pismo Beach's dark skies. Elevation of the observer likewise had little if any perceivable effect: antitwilights observed at sea level were largely indistinguishable from those seen from mountains as high as 1300 m (Bureau of Land Management land in Inyo County and Death Valley National Park). The only visually obvious parameter that influenced the antitwilight was the aerosol load. Hazy skies muted the colors, so we always made measurements when the sky was judged to be very clear.

3. PHOTOGRAPHIC AND VIDEO OBSERVATIONS

Using "visually very clear and cloud-free" as our visual criterion for observations, we took digital still photographs and time-lapse movies of the antisolar twilight from a number of locations: Will Rogers State Beach in Los Angeles, Westward Beach in Malibu, California, and Oceano Dunes State Vehicular Recreation Area near Pismo Beach, California. A GoPro Hero Black video camera was mounted in a fixture containing bubble levels, an inclinometer, and a compass so that azimuth and altitude of the center of the frame could be adjusted and recorded. This was done so that later we could overlay azimuth and altitude grids that we computed using software developed specifically for this purpose. Still cameras were a Pentax Kx and a Nikon AW100. With very minor exceptions, both cameras recorded imagery that looked the same as our visual observations. All photographs presented here were taken looking westward over the ocean during morning twilight to avoid urban lights.

Still photographs and videos were analyzed using their RGB colors as proxies for irradiance. RGB values are related to irradiance through monotonic transfer functions that preserve the relative brightnesses of each color. The occasional and infrequent white balance changes made automatically by the video cameras were found to have negligible effects on the RGB values relative to
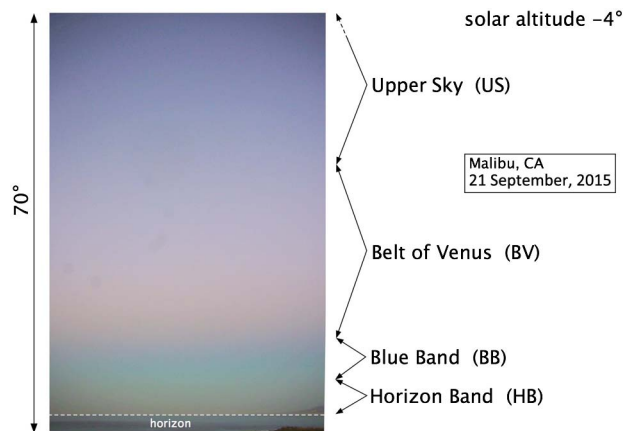
one another. Our impression is that RGB videos and photographs accurately captured the scene as we saw it by eye. Therefore we chose to use RGB rather than go through the enormous effort of radiometrically calibrating thousands of video frames. For related results based on calibrated still photographs, see Lee [9–12].

Observational results reported here refer to clear skies in the northern mid latitudes (about 35° N) during autumn and winter, though experience shows that they are the same throughout the year. Most of our observations were done at sunrise, so our narrative will assume that the Sun is rising, though obviously the twilight phenomenology is essentially the same at sunset but reversed in time.

4. ANTITWILIGHT PHENOMENOLOGY FOR A SEA LEVEL OBSERVER

Figure 1 shows a photograph of the antitwilight looking west over the Pacific Ocean just before sunrise when the Sun was 4° below the horizon. It has been slightly enhanced to render the antitwilight's structure easier to see. Four roughly horizontal bands are evident (Table 1). They and their abbreviations are (1) upper sky (US), (2) Belt of Venus (BV), (3) blue band (BB), and (4) horizon band (HB). Question marks "?" indicate uncertainty on our part as to what part of the antitwilight earlier authors are referring to.

The terms "upper sky," "blue band," and "horizon band" are new descriptors chosen based purely on observation. This approach avoids terms like "shadow of the Earth," which, in some cases technically correct and widely known, implicitly invokes an interpretation. Wide-angle photographs show that the diffuse boundary between the BV and BB is slightly concave down so the historic term "arch" is geometrically correct [13,14]. The curvature of the "arch" is subtle and generally not obvious to the visual observer.

Figure 2(a) shows a time sequence of images from a video of the antitwilight sky as the Sun rises. Figure 2(b) (Visualization 1) shows the complete video. Figures 3(a) and 3(b) show vertical RGB brightness profiles extracted from the video [Fig. 3(c), Visualization 2] set against an "image" of the antitwilight. The background "image" in Fig. 3 is based on 10 vertical columns of pixels from Fig. 1 (width approximately 0.6°) that were horizontally averaged in R, G, and B. This was done to reduce pixelation noise. The resultant average color at each altitude was then used to reconstruct the background image that quantitatively reproduces the original antitwilight photograph.

Fig. 1. Slightly color-enhanced still image of the antitwilight when the Sun was at an altitude ε of –4°. Four bands can be seen, and they are indicated on the right. Photo taken 21 September 2015 from Westward Beach in Malibu, California, USA (34.011899, –118.818028).

Table 1. Four Visual Components of the Antitwilight: Historic and Revised Terms

Revised Term (This Work)	New Abbreviation	Minnaert [3]	Neuberger [4]	Lee [11,12]
Upper sky	US	Blue? Bright reflection?		
Belt of Venus	BV	Counter-twilight	Antitwilight arch	Belt of Venus Antitwilight arch Upper antitwilight arch
Blue band	BB	Earth-shadow	Dark segment	Dark segment Earth's shadow
Horizon band	HB	Lower counter twilight? Lowest counter twilight? Second faint Earth shadow?		Dim reddish band? Lower antitwilight arch

Fig. 2. (a) Shows a sunrise time sequence of the antitwilight from the video (b) (Visualization 1). Field-of-view (FOV) of each frame is 118° × 69°. The view is westward over the Pacific Ocean, and it was cold and clear at sunrise. Refracted solar altitude ε is shown in each frame. The video was taken in the time-lapse mode with a 2 s frame interval. When played back at 30 frames/s, time compression was 60∶1, resulting in 1 s of video time = 1 min of real time. The video was taken with a GoPro Hero 4 Black on 31 December 2015 from Oceano Dunes State Vehicular Recreation Area (35.106070, –120.630673) near Pismo Beach, California, USA. The complete video can be found in (b) (Visualization 1—GOPR1412.MP4).

A. Overall Brightness Structure

There are three key findings relating to the gross structure of the antitwilight.

(1) For $-6° < \varepsilon < -3°$, the positions of the upper sky (US) and horizon band (HB) remain fixed, while the blue band (BB) and Belt of Venus (BV) change position over time. The color and brightness of the HB changes with solar altitude, as we will discuss in Section 4.E.

(2) The altitude of maximum sky brightness increases ∼linearly downward toward the horizon until it reaches a maximum, then decreases toward the horizon. These maxima are generally less than at 10° altitude and decrease at the same rate that the Sun rises (Fig. 4). For $-6° < \varepsilon < -3°$, blue is the brightest of the RBG colors at every altitude, but when $\varepsilon > -3°$, red light from the BV becomes and remains the brightest component.

(3) The width of the transition between the BV and BB decreases linearly as the Sun rises (Fig. 5), from about 8° when $\varepsilon = -3°$ to 0.9° when $\varepsilon = 0°$.

Figure 3 shows that the antitwilight contains significant amounts of all three RGB colors. As such, the colors are pale, unsaturated, and certainly not narrow band like an emission line. Despite visual descriptions of rich colors, Lee [9–12]

has shown that during civil twilight the colors of vertical scans through the antitwilight span only a small region of u' and v' space near the achromatic point in the 1976 CIE color diagram.

B. Upper Sky

The US is blue and reaches up to the zenith. It represents the background atmosphere and is always visible during twilight. Down to around $\alpha = 10°$ all three RGB color profiles are more or less parallel to one another until the BV becomes prominent around $\varepsilon = -3°$ (Fig. 3). Before sunrise, the US is decidedly blue. It becomes progressively grayer (less blue) until it is only slightly bluish at $\varepsilon = -2°$, where the R, G, and B curves around $\alpha = 60°$ almost merge. As the Sun continues to rise, the US grows progressively more blue as the R, G, and B curves separate through sunrise. The US's color, judged by eye, seems to be the same color as daytime skies [15, 16], slightly modified by illumination from the Sun-side (opposite) twilight.

C. Belt of Venus

Below the US is the Belt of Venus. It is bounded diffusely above by the US and more sharply below by the BB. It is generally described as "pink," though the color varies with the elevation of the observer, altitude of the observer's line-of-sight (LOS), and aerosol load. The BV first becomes visible when ε is about –6°, though it is not apparent in the photographs or videos until about –5°. It is always brighter in its lower portions. Roughly speaking, the BV and BB represent the sunlit and shaded portions of the atmosphere, respectively. They are inseparable and move together.

At around $\varepsilon = -4°$, the BV starts to become bright enough to influence the overall sky brightness and structure. By $\varepsilon = -2°$, it is the brightest part of the antitwilight, remaining so until sunrise. At $\varepsilon = -2°$ and –1°, there is a slight upturn in the R curve within a few degrees of the horizon in our measurements. We do not understand this, but we speculate that it could be due to multiple scattering contributions.

As has been frequently mentioned in the literature [3–7], the altitude of the BV changes much more rapidly than the solar altitude does. Sometimes it is the "shadow of the Earth" that is described. The effect is evident in Figs. 2 and 3. Though not explicitly specified, we presume that the authors are referring to the lowest, brightest part of the BV, as it transitions to the BB. This movement will be discussed in greater detail in Section 6.

D. Blue Band

Below the BV is the blue band. It is generally a shade of blue but it can take on greenish or turquoise hues depending on altitude and solar altitude, and aerosol load. It moves downward with the BV as the Sun rises. Its vertical extent also decreases as the Sun rises. The BB first becomes evident when the BV appears, almost by definition, since it is the color contrast between the two that makes the boundary visible. It is visible from about $\varepsilon = -6°$ until $\varepsilon = -1°$, though it sometimes seems to persist for a few minutes after sunrise, a topic we will investigate in Section 9.

E. Horizon Band

The horizon band is below the BB, is always visible, and is firmly anchored to the horizon. Colors in the HB may initially
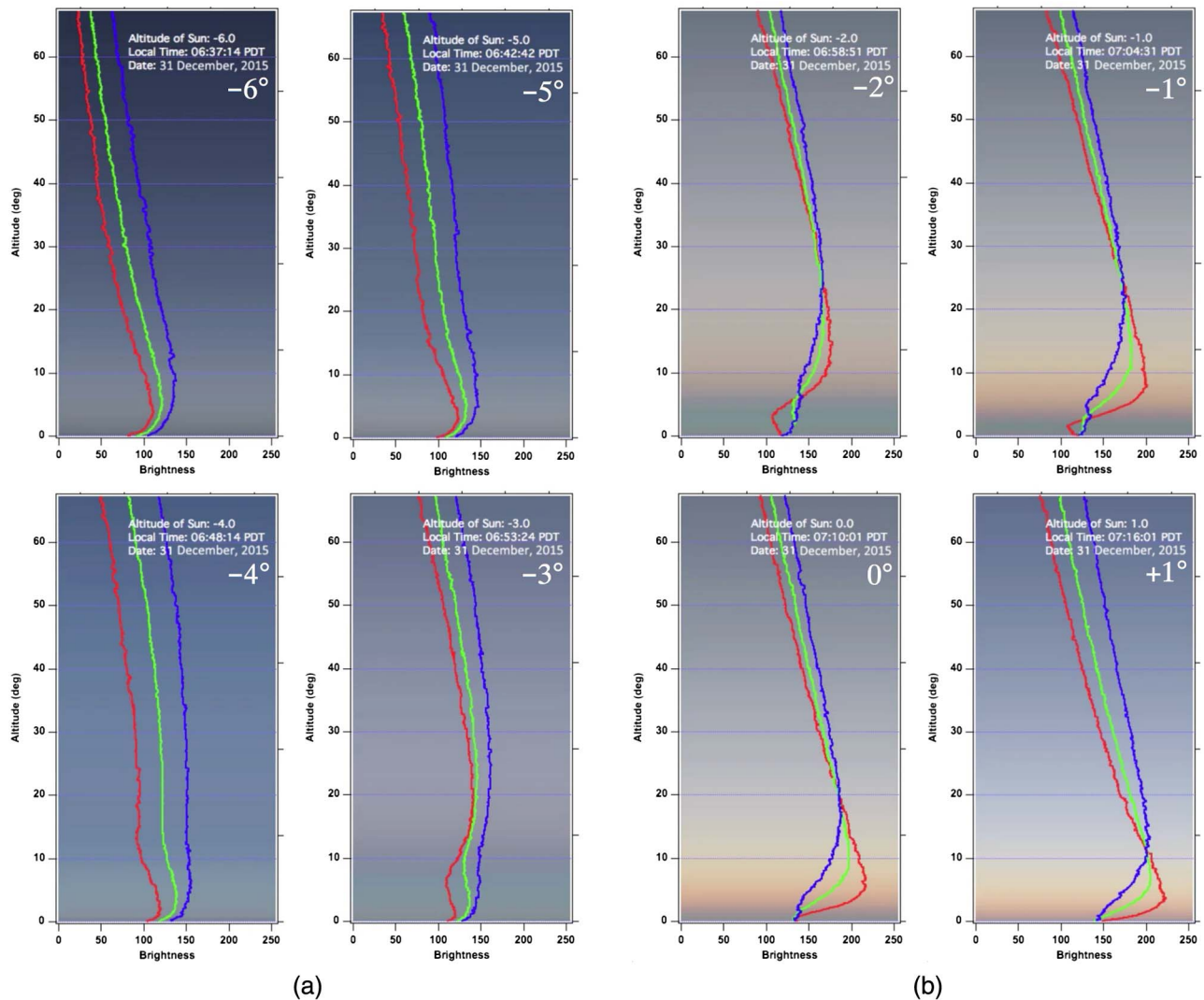
Fig. 3. (a) and (b) Reconstructed images of the antitwilight based on the colors of the vertical profiles from the video (Fig. 2). Refracted solar altitude ε is shown in the upper right-hand corner of each image. The complete video can be found in (c) (Visualization 1—Dawn 1 copy).
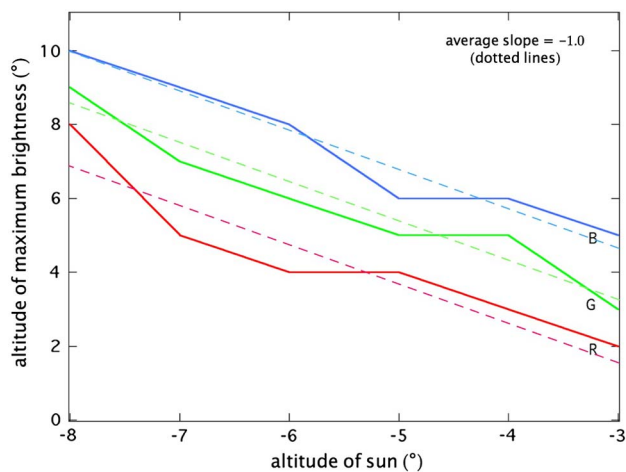

Fig. 4. Altitude α of the relative maximum brightness (solid lines) versus solar altitude ε for each color R, G, and B. Data from video [Fig. 3(c)]. The dashed lines indicate that the observations follow linear trends.

be gray, blue, or faintly reddish, but they change dramatically during twilight. When the Sun reaches around –4°, the BB enters the HB and colors it blue. Around $\varepsilon = -2°$, the HB's color becomes pink as the BV enters it, and it remains pink until after sunrise.

F. Shadow of the Earth Visible After Sunrise?
As a prelude to Section 8, Figs. 2 and 4 show that there is a dark band hugging the horizon after sunrise. It is about 3° in vertical extent, measured upward from the horizon. This feature is often called the "dark segment (DS)" or "shadow of the Earth." Yet how can a shadow opposite the Sun be visible when the Sun is above the horizon? [8] In view of the confusion in the literature as to what constitutes the dark segment and its optical origin, it is worth taking a closer look (Fig. 6).

As the altitude of the Sun goes from –1° to +1°, the color of the dark segment, i.e., the color of the sky immediately above the horizon, changes. When $\varepsilon > 0°$, the dark segment is reddish due to light that one associates with the BV, which after
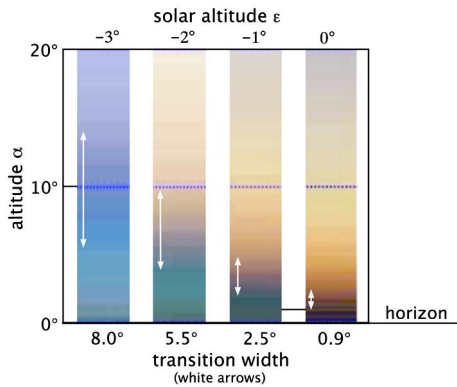
Fig. 5. Approximate vertical width of the transition zone between the BB and BV estimated by eye from Fig. 3. Colors are enhanced. Widths of the transition regions are given below the images.
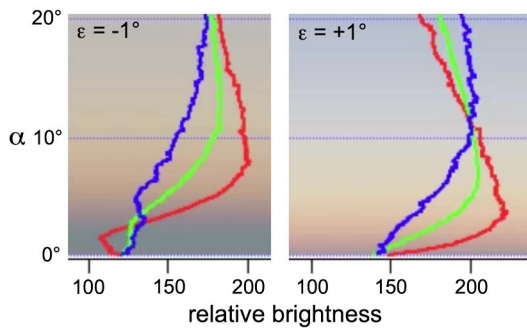
**Fig. 6.** Details of the horizon sky colors from Fig. 3.

Table 2. Antitwilight Bands as a Function of Solar Altitude ε[a]

$\varepsilon°$	Phenomenology
−6°	BV barely discernable by eye. Top of HB 15°. Bottom of BB imperceptible.
−5°	Top of HB 9°. Top of BB 35°. BV evident 35°–80°.
−4°	Top of HB 6°. Top of BB 25°. BV 25°–60°.
−3°	Top of HB 3°. Top of BB 13°. BV 13°–50.
−2°	HB gone, replaced by BB. Top of BB 8°. BV 8°–40°. BV brightest part of antitwilight.
−1°	BB 0°–2°. BV 2°–30°. BV brightest part of antitwilight.
0°	BB gone. BV 0°–25°. BV brightest part of antitwilight.
+1°	BV 0°–25°, touching horizon. BV brightest part of sky.

[a]Based on observations presented in Figs. 2–6 and shown schematically in Fig. 7.

sunrise, sits on the horizon. Note that for −1° < ε < +1°, the three color curves coincide at the horizon, and the HB here is "gray."

Based on Figs. 1–5, Table 2 summarizes the main twilight features and their changes throughout morning twilight. Figure 7 shows the antitwilight phenomenology graphically. Indicated solar altitudes are accurate to about 0.1°, and band structure altitudes are approximate, accurate to within about 10%. Constructing this diagram was done by visually inspecting and measuring the photographs and videos. Such an
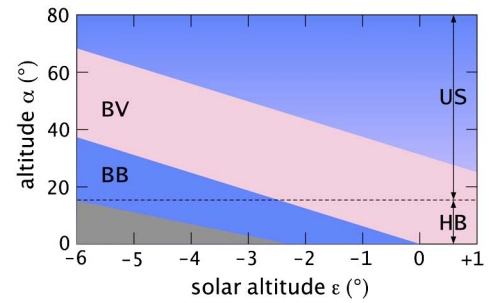
Fig. 7. Representative antitwilight map showing observed band altitudes α as a function of solar altitude ε. (prepared from the average of Pismo and Malibu observations) This diagram corresponds to our observations and will be a little different for each antitwilight. As the Sun rises, the BV and BB descend rapidly, each reaching the horizon in order. The bands move downward about eight times faster than the Sun rises. Although the HB stays fixed within the lowest 15° of the sky (horizontal dashed line, see Section 5), it turns blue when the BB reaches it around −2,° then it turns pink as the BV settles on to the horizon. The boundaries between bands are never sharp. As discussed in Appendix A, the altitudes of twilight phenomenology vary with the clarity of the observer's atmosphere and his elevation.

approach is fraught with perceptual biases because any area of color is perceived in relation to adjacent colors. For example, even though the Belt of Venus appears to be reddish at ε = −3°, the RBG profiles show that it contains more blue light than red.

G. Summary of Antitwilight Phenomenology

We remind the reader that the observations and interpretations reported here are for our observations at sea level during autumn and winter looking west over the Pacific Ocean. Observers at other locations will encounter different atmospheric and illumination conditions. Although our visual observations were made under a variety of conditions and elevations, our experience is that clear sky antitwilight phenomena are all very similar and that what we have reported above is typical.

5. PHYSICAL OPTICS OF THE ANTITWILIGHT IN A PURE RAYLEIGH ATMOSPHERE

A. Preliminary Remarks

The blue color of the upper sky would seem to be explainable by Rayleigh scattering alone but in fact some of its color is the result of ozone absorption in the Chappius bands [17,18]. In this and the following sections, however, we shall assume that scattering of sunlight by air molecules is the only interaction. In so doing, we ignore absorption by ozone and other molecular species.

Consider the path of a photon that underdoes single scattering in the antitwilight sky before reaching the observer. Figure 8 shows that the path length from the Sun to the point of scattering is much greater than the path length from the point of scattering to the observer's eye. For a rough numerical example, an unrefracted ray traveling horizontally from a sea level observer passes through 450 km of atmosphere that is 16 km thick (two density scale heights), while scattered light must originate from within the atmosphere, which is generally
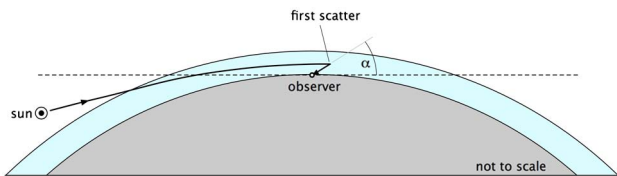
Fig. 8.　Geometry of singly scattered sunlight. The path length from the Sun to the first scatter is always much greater than the path length from the first scatter to the observer. Thus, the color and brightness of sunlight reaching the antitwilight sky is almost entirely determined by the transmitted sunlight before the first scatter occurs.

only about 16 km away. Therefore the color and brightness of light illuminating the antitwilight quadrasphere—and ultimately reaching the observer—is primarily determined before the scattering takes place.

Regardless of the illumination (day, night, twilight), there are two visually distinguishable parts of the sky corresponding roughly to the upper sky and horizon band: (1) the upper sky is blue and optically thin, while (2) the lowest few degrees are whitish and optically thick. These two regions are the canvas upon which the antitwilight is painted. The upper sky color and brightness is due to Rayleigh scattering in an optically thin atmosphere that grows thicker (hence brighter) as the LOS moves to lower altitudes. The maximum brightness occurs where the observer's LOS starts to become optically thick, below which (2) it grows dimmer down to the horizon, a complicated radiative transfer effect as discussed by Lee [9,12].

Light of any wavelength reaching the observer during twilight tends to come from optical depth (τ) of unity at that wavelength. Broadly speaking, when $\tau < 1$, only single scattering takes place. When $\tau > 1$, multiple scattering will occur. Depending on the LOS altitude α and wavelength λ, the atmosphere may or may
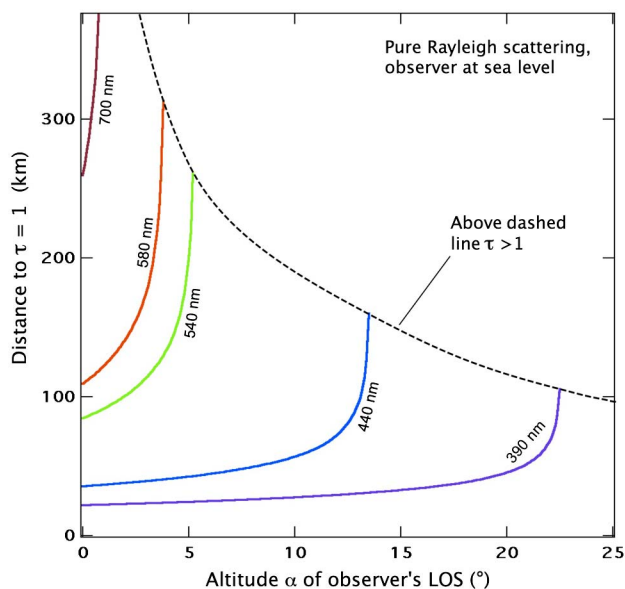
Fig. 9.　For a pure molecular atmosphere, the distance from the sea level observer to the point where the optical depth is unity is a strong function of wavelength due to the $1/\lambda^4$ dependence of Rayleigh scattering. Refraction included in the calculations.

not be optically thick. Figure 9 shows the distance from a sea level observer to optical depth unity for a variety of wavelengths in a pure Rayleigh atmosphere. The distance from the observer at which $\tau = 1$ will occur at different distances at different wavelengths, with longer wavelength reds coming from much farther away than the shorter wavelength blues owing to the strong wavelength dependence of the Rayleigh scattering cross section ($1/\tilde{\lambda}$). Note that at an LOS altitude α of 5°, the sky is optically thick at wavelengths shorter than 500 nm (green) and optically thin at longer wavelengths.

For a sea level observer, optical depth unity occurs at an LOS altitude of around $\alpha = 5°$ (10.5 air mass) at 540 nm in a pure Rayleigh scattering atmosphere, the clearest possible sky. The LOS altitude of $\tau = 1$ will decrease with increasing (aerosol) opacity in the Earth's boundary layer. For our observations, the average (broad band) optical depth of unity occurred at around 15° (Appendix A), indicating some but not extreme aerosol loading.

B. Overall Brightness Structure

The observer can see the shadow of the Earth cast upon the atmosphere whenever the Sun is below the horizon. In our terminology, the shadow encompasses the blue band and the horizon band.

Figures 10–12 are schematic diagrams of antitwilight phenomena for three representative Sun altitudes ε. They are drawn with no atmospheric refraction and with the Sun as a point source. The geometrical boundary between the sunlit and shaded atmosphere is here called the *shadow line* [19]. It is obviously a cylindrical surface in 3D, but in 2D cross section it can be represented as a line.

For $\varepsilon < -4°$, (i.e., −5, −6, −7, etc.) the maximum brightnesses in the vertical profiles of Figs. 3(a), 3(b), and 4 occur near or slightly below the point at which the observer's LOS becomes optically thick ($\alpha = 15°$), though, as mentioned in Section 5.A, optical depth is a function of wavelength. The decrease in brightness near the horizon occurs for two reasons. (1) The air mass increases downward toward the horizon as the LOS passes through progressively more atmosphere, and hence sunlight is lost to scattering. (2) Once the LOS reaches the shadow line between the BV and the BB, the atmosphere below it is in shadow and thus receives less sunlight. Both bands show the ever-present dimming of the sky near the horizon due to multiple scattering and extinction, as described by Lee [9,10].

C. Upper Sky

The US and HB are faintly visible all night due to starlight, moonlight, and airglow (Fig. 10). Both become quite evident when astronomical twilight begins at $\varepsilon = -18°$. But when does direct sunlight first illuminate the US? From Fig. 10, it is obviously when the shadow line first intersects the "top of the atmosphere" (TOA). But there is no sharply defined TOA because the atmospheric density decreases exponentially upward. Sunlight scattered from high in the atmosphere might be visually detectable because the Sun is so bright. So we shall turn the question around and ask, "When is sunlight directly scattered from the US first detectable by the observer?" Observationally, it is at or just before the BV first appears,
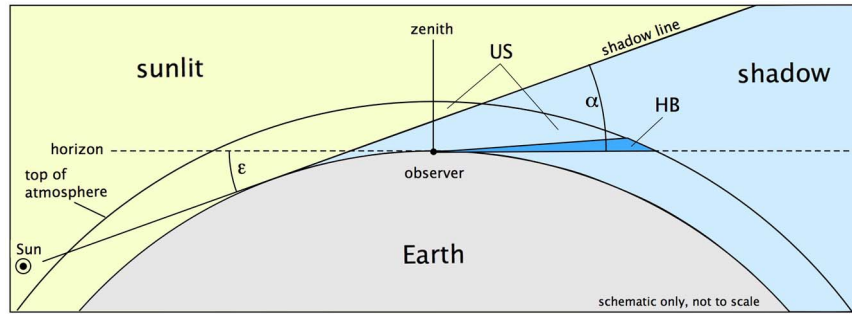
Fig. 10. When the Sun is below about –8°, only the HB and US are evident. The observer's LOS through the antitwilight is mostly in shadow but may pass through sunlit atmosphere at higher altitudes.
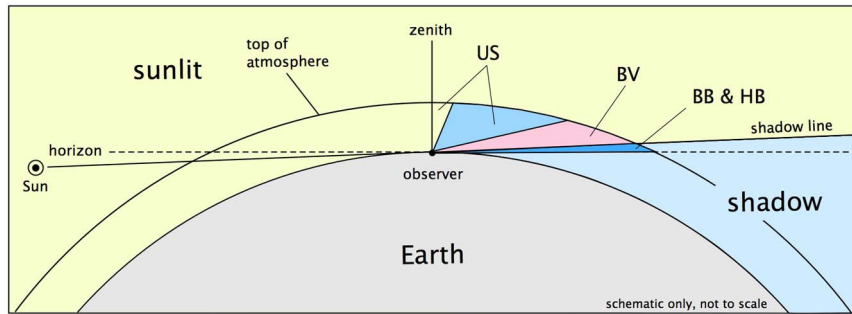
Fig. 11. When the Sun is above –8° the BV starts to appear, along with the BB.
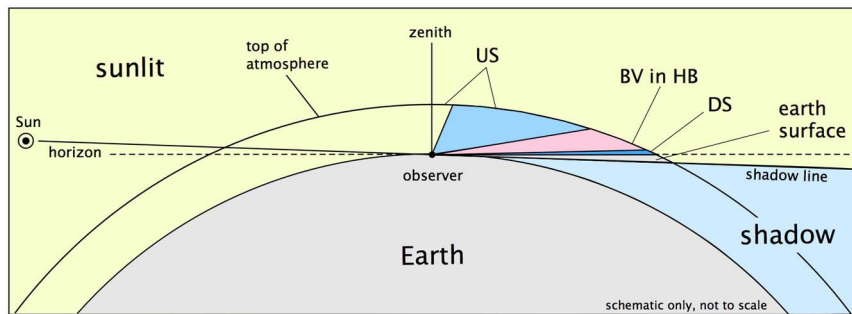
Fig. 12. At sunrise, the BV occupies the HB, and the is BB gone. The dark segment DS is visible just above the horizon.

at $\varepsilon \approx$ –6°, when the upper part of the BV is about 70° altitude. Working out the geometry of Fig. 10, the effective TOA is then about 36 km elevation, in the stratosphere.

When $\varepsilon >$ –6°, the observer's LOS passes through shaded and sunlit parts of the antitwilight atmosphere. Before the BV appears, those parts of the US that may be sunlit occur so high in the atmosphere (in both an angular and elevation sense) that they contribute little to sky brightness because the air is so thin. When $\varepsilon =$ –2°, the HB's gray light is replaced by blue light from the BB down to the horizon. Hints of the BB are present, but as explained in Section 4, it is distinguishable as a separate band only when the BV is present.

D. Belt of Venus

The Belt of Venus initially comes from the optically thin atmosphere that is illuminated by direct sunlight. Its upper boundary is

diffuse and ill defined. Light from the BV is predominantly blue between –6° and –3°, though it appears pinkish due to contrast with the BB and US [Fig. 3(a)]. Beginning at $\varepsilon =$ –2°, the BV begins to have more red light than blue and remains the brightest part of the antitwilight [Fig. 3(b)]. This is due primarily to the lowest and brightest parts of the BV having entered the optically thick portion of the LOS, the HB, and therefore strongly scatters ("reflects") incident light. The BV's pink color is a consequence of the yellowish or reddish low Sun illuminating air molecules, and the scattered light's color is modified by Rayleigh scattering, adding blue to it. As is well known, red and blue together produce purple and pink is bright purple.

E. Blue Band

When the Sun is below about –4°, both BB and HB are in the shadow of the Earth. The BB's vertical extent decreases as the

Sun rises. Its rich blue color is a consequence of both multiple Rayleigh scattering and optical depth effects. When the solar altitude is less than about 15°, the BB (in our observations) was always optically thick. Thus, multiple scattering is important here. Rayleigh scattering modifies white sunlight by $1/\lambda^4$, and with each successive scattering, the light becomes progressively bluer. Being adjacent to the pink BV, the BB's color is accentuated even more.

Because the observer's LOS is oblique to the shadow line, the width of the boundary between the BV and the BB is always diffuse (Fig. 5) and grows smaller as ε approaches zero. The decrease as the Sun rises (Fig. 5) is a geometrical effect (Fig. 13). The observer's oblique LOS through the shadow line becomes progressively more parallel to the shadow line as the Sun approaches the horizon, i.e., as ε approaches 0°. As a result, the angular width of the transition region decreases. Geometrically, when the Sun is on the horizon, the angular width of the transition zone is the same as the angular diameter of the Sun (1/2°), though optical depth effects in the low LOS may modify its width somewhat.

F. Horizon Band

The horizon band is primarily due to the observer's optically thick LOS. Being opaque, the atmosphere multiply scatters all colors with roughly equal efficiency. Thus, it is intrinsically "white." Therefore, its color depends on the color of the light that is illuminating it. First the BB makes it blue, then the BV makes it pink at sunrise.

As previously mentioned, the HB has seldom if ever been recognized as a separate and distinct twilight feature (Table 1). This is probably because it is so low on the geometrical horizon, i.e., near 90° from the zenith. While easily visible over the ocean with clear skies, even a slightly elevated local horizon (skyline) due to hills or trees can block it from view. Also, it takes only a little haze to make it difficult to distinguish the HB from the BB. As shown in Appendix A, the altitude of the boundary between the BB and HB depends on the clarity of the atmosphere.

6. ALTITUDE OF THE BELT OF VENUS AS A FUNCTION OF SOLAR ALTITUDE

Figure 13 shows vertical slices through the twilight as a function of solar altitude. Each is centered on the horizon opposite the Sun. Most evident is the fact that the boundary between the Belt of Venus and blue band sets much more rapidly than the Sun rises. The boundary decreases by dozens of degrees even though the altitude of the Sun changes by only 2°–3°. This effect has been frequently reported in the literature [3–7]. The vertical width of the HB also decreases as the Sun approaches the horizon from below (Fig. 5).

To analyze the relation between solar altitude and bottom of the Belt of Venus (first performed by Pertner and Exner [20]), consider Fig. 14. It shows the geometrical circumstances relating to the shadow line in the antisolar twilight in the absence of refraction and treating Sun as a point source. With the Sun at an altitude $-\varepsilon$, the shadow line is tangent to the Earth's surface at $P(x_p, y_p)$ and it defines the upper edge of the shadow. The
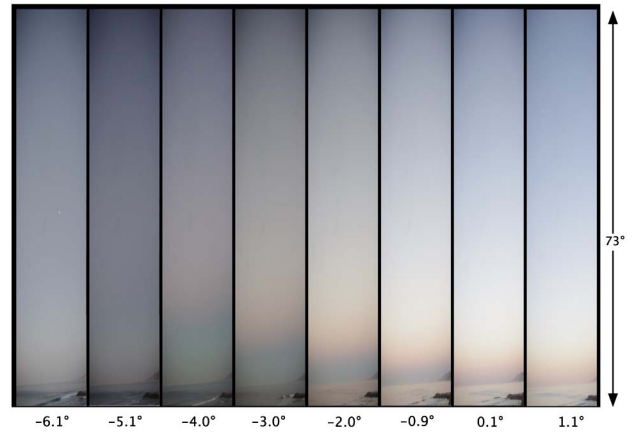
Fig. 13. Vertical strips through the antitwilight as a function of the solar altitude ε for a rising Sun. Note how rapidly the boundary between the Belt of Venus and blue band drops toward the horizon as the Sun rises. All four bands are best seen when $\varepsilon = -4°$. When $\varepsilon = -2°$, the HB is blue because the BB occupies it. When $\varepsilon = +1°$, BV has reached the horizon so the HB is pink. See Figs. 3–6 for more quantitative measurements.

shadow line also intersects the top of the atmosphere (TOA) at T.

The equation of the shadow line in Cartesian coordinates with the origin at the observer O through a tangent point $P(x_p, y_p)$ on the Earth's surface is

$$y = mx - mx_p + y_p, \tag{1}$$

where m is the line's slope ($= \tan \varepsilon$). The location of $P(x_p, y_p)$ is

$$x_p = -R \sin(\varepsilon),$$
$$y_p = R \cos(\tilde{\varepsilon}). \tag{2}$$

The equation for the TOA is

$$x^2 + (y + R)^2 = (R + H)^2, \tag{3}$$

where H is the density scale height, a reasonable first-order estimate of the height of TOA. H is about 8.5 km. To locate $T(x_T, y_T)$, we eliminate y between Eq. (1) and (3) to get

$$x^2 + (mx + L + R)^2 - (R + H)^2 = 0, \tag{4}$$

where L and K are constants

$$L = x_p - y_p/m = -R \sin(\varepsilon) - R \cos(\tilde{\varepsilon}m + R/m), \tag{5}$$

$$K = L + R. \tag{6}$$

Equation (4) is quadratic in x and has two solutions, only one of which is relevant to T. After solving Eq. (4) and computing the coordinates of $T(x_T, y_T)$, we can calculate the angle α,

$$a = \tan^{-1}(y_T/x_T). \tag{7}$$

Figure 15 shows the solutions for $\alpha(\varepsilon)$ for scale heights $h = 8$ km, 16 km, and 32 km. In comparing them to Fig. 13, we see a qualitative match, in the sense that α increases much faster than ε does. Figure 15 also shows that $\alpha \geq -\varepsilon$ for all values of $\varepsilon < 0$, and indeed α rapidly approaches 90° (zenith) when ε is still in single digits. Only for $\varepsilon = 0$ is $\alpha = \varepsilon$.
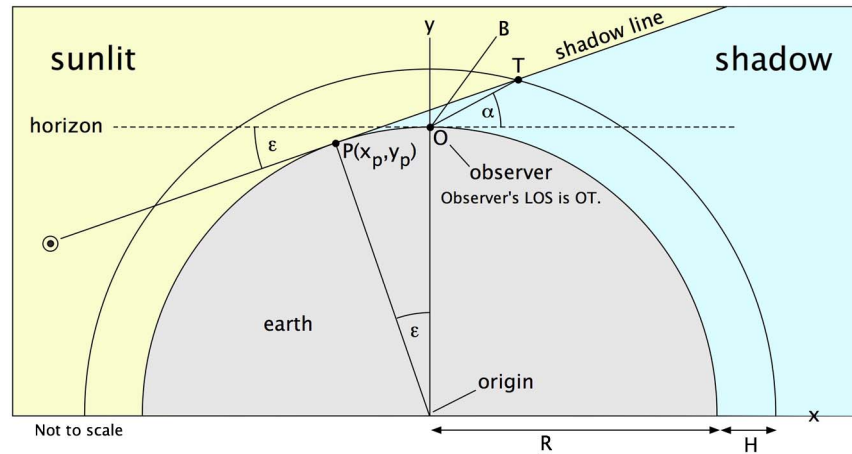
Fig. 14. Geometry of the shadow line relative to the observer. No refraction is included.
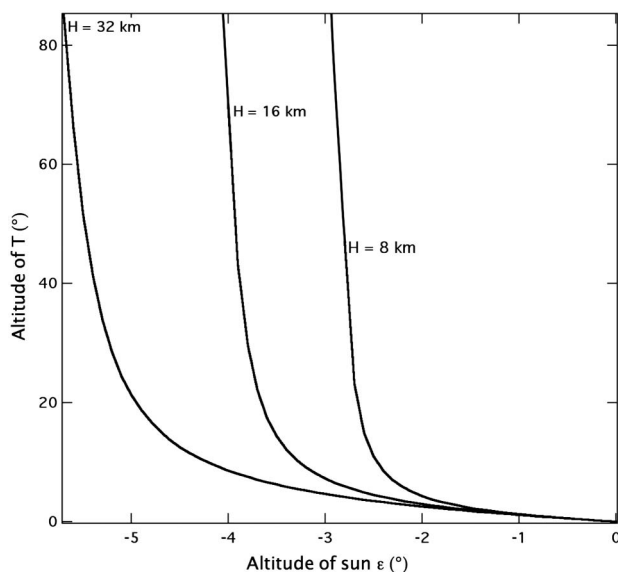
Fig. 15. Geometrical computation of the altitude α of the intersection of the observer's line-of-sight with the top of the atmosphere T as a function of solar altitude ε for three density scale heights h. When the Sun is near the horizon, α changes slowly but quickly accelerates upward as ε becomes more negative. For example, if $h = 16$ km, α is about 8° for $-3° < \varepsilon < 0°$ but reaches almost 90° by the time ε has reached $-4°$.

Yet α, the altitude of T, which lies on the shadow line, is not the same as the altitude at which the observer sees the boundary between the BV and BB. When observers estimate the altitude of the boundary [3,17], the relationship found is essentially linear with solar altitude (Fig. 16), and not highly curved as Fig. 5 shows. As observers have reported, however, the altitude is a steeply sloping function of ε. Figure 16 shows that the boundary altitude varies roughly 8 times as fast as ε.

Regarding color, Figs. 3 and 13 show that light of the upper sky has a faint reddish component from the BV that increases until around $\varepsilon = -2°$ when the R, G, and B curves are as close together as they ever get, especially at higher altitudes. Thus the
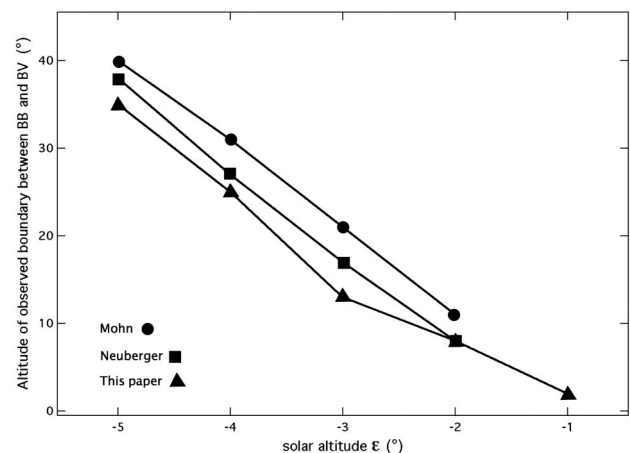

Fig. 16. Measured altitude α of the blue-to-pink transition between the Belt of Venus and blue band as a function of solar altitude ε. Mohn data [20] reported by Neuberger [4], Neuberger data from Neuberger [21].

sky becomes almost gray, but becomes bluer toward sunrise (the R and B curves separate). The red component comes from the BV, which of course is reddish because the low Sun is reddish. We can use Fig. 14 and Eqs. (1)–(7) to learn where in the atmosphere this reddish light originates. Rather than select a value for H and solving for α, we select a value of α and ε, and solve for H. For α and ε of 60° and $-4°$, respectively, we find H to be about 37 km (stratosphere), and for α and ε of 60° and $-2°$, respectively, $H = 4$ km (troposphere).

The LOS through the BV-BB boundary passes obliquely through the shadow line and its integrated brightness is weighted by brightness and transmission through the atmosphere. As Fig. 14 shows, an LOS labeled OB can pass through both shaded and sunlit atmosphere and thus the LOS brightness will be influenced by each part.

Figure 17 provides a physical explanation as to why $\alpha(\varepsilon)$ changes so rapidly. Using the same geometry as Fig. 14, consider the situation where two solar altitudes are depicted, one $(\varepsilon_1, \alpha_1)$ that is twice as large as the other $(\varepsilon_2, \alpha_2)$. For the
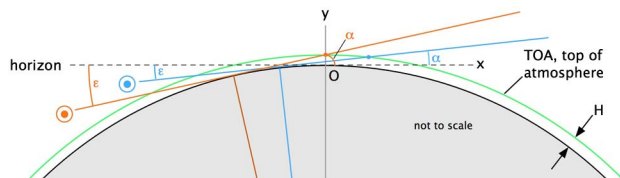
Fig. 17. Rapid increase in α as ε goes more negative is a geometrical effect due to the small thickness of the atmosphere compared to the radius of the Earth. For the smaller value of ε, α is also small (ε_1, α_1). But when ε is twice as large, α becomes 90° (ε_2, α_2)). Thus, as ε grows more negative, α rapidly increases.

smaller value of ε, α is also small. But when ε is twice as large, α becomes 90°. This is a geometrical effect due to the relatively small thickness of the atmosphere compared to the much larger radius of the Earth: 8 km versus 6371 km. If H were larger, α would increase more slowly, as Fig. 17 shows.
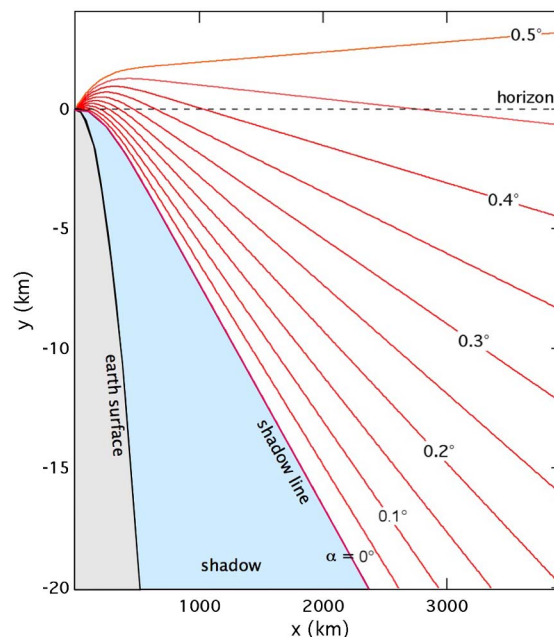
7. REFRACTION

Normal atmospheric refraction shifts the apparent location of a celestial body upward from its true geometric position. The effect is strongest near the horizon in the HB where objects may appear elevated by more than half a degree. Such refraction causes the Sun and Moon to appear just above the horizon when geometrically, i.e., in the absence of the atmosphere, they are below the horizon. The maximum amount of refraction for a normal atmosphere is about 35 arcmin (0.58°) [22,23]. Throughout the year, the angular diameter of the Sun varies from 0.525° to 0.543°. For the Moon, the range is 0.489°–0.568° monthly. Thus, when either body appears just touching the horizon, they are geometrically below the horizon.

To account for refraction, we ray traced various LOS trajectories through the atmosphere. The technique was to launch a ray from the surface of the Earth with a fixed segment length of 1 km, then refract it by the amount dictated by the difference in the index of refraction at the segment's starting and ending points. The refracted trajectories were validated against other methods that use fixed atmospheric shell thicknesses, another standard approach. The path differences between the two techniques were negligible. Figure 18 shows trajectories of light rays along the observer's LOS for various altitudes between $\alpha = 0°$ (horizontal LOS) and 0.5°. Note that most of the rays are refracted and ultimately pass below the geometrical horizon but never strike the Earth. At $\alpha = 0°$, the ray is always below the horizon and always above the surface of the Earth. Since the horizontal ray ($\alpha = 0°$) defines the shadow line for $\varepsilon = 0°$, a sea level observer can never see into the shadow of the Earth.

Note that the observer can never see far enough in a pure Rayleigh atmosphere to actually see below the horizon because the optical depth is too large (Fig. 9). The fact that the Sun and Moon can be seen at such low LOS altitudes is because they are so bright that some of their light gets through.

8. DARK SEGMENT

As shown in Figs. 2, 3, 5, and 6, after sunrise there is a dark region of the sky about 3° high just above the horizon and

**Fig. 18.** Ray traces through the atmosphere for an observer on the surface for LOS altitudes α from 0° (horizontal) to 0.5° above the horizon. For these very low altitude angles, refraction bends the ray from below the horizon. Thus, the light an observer sees looking slightly above the horizon originates from below the horizon. For a horizontal LOS ($\alpha = 0°$), the refracted ray defines the shadow line when the Sun (as a point source) is on the refracted horizon. In this case, the observer's LOS can never reach into the shadow.

touching it. This feature is usually called the "dark segment" [24]. It is often identified with the "shadow of the Earth" before sunrise. To an observer, it seems to be continuously visible from before sunrise until a few minutes after sunrise. There is some variation in the literature as to how the dark segment is defined observationally, and its optical origin [25].

To understand it, we must look at the time evolution of light coming from the lowest few degrees above the horizon. First, the BB reaches the HB where it is darkest just above the horizon. Then the BB is replaced by the BV when ε is approximately –0.5°, at which point the DS becomes evident and is visible for a short time (minutes) after sunrise. Both being dark, the logical assumption is that they are the same phenomenon. As mentioned in Section 4.F, after sunrise the DS is reddish due to the BV. But the shadow of the Earth, by definition, is blue. So how can the "shadow of the Earth" be seen when the Sun is above the horizon? And is the dark segment the shadow of the Earth? Figure 19 reveals the answers.

Figure 19(a) shows the simplest case of shadow geometry when the observer sees the Sun on the horizon. In this case, we treat the Sun as a point source for clarity. When the observer's LOS is horizontal, the LOS is refracted downward and defines the shadow line. He cannot see the shadow because to do so would require him to look below the geometrical horizon where the shadow would then be blocked from view by the Earth.

Now consider the case where the Sun is no longer a point source and appears above the horizon with its lower limb just
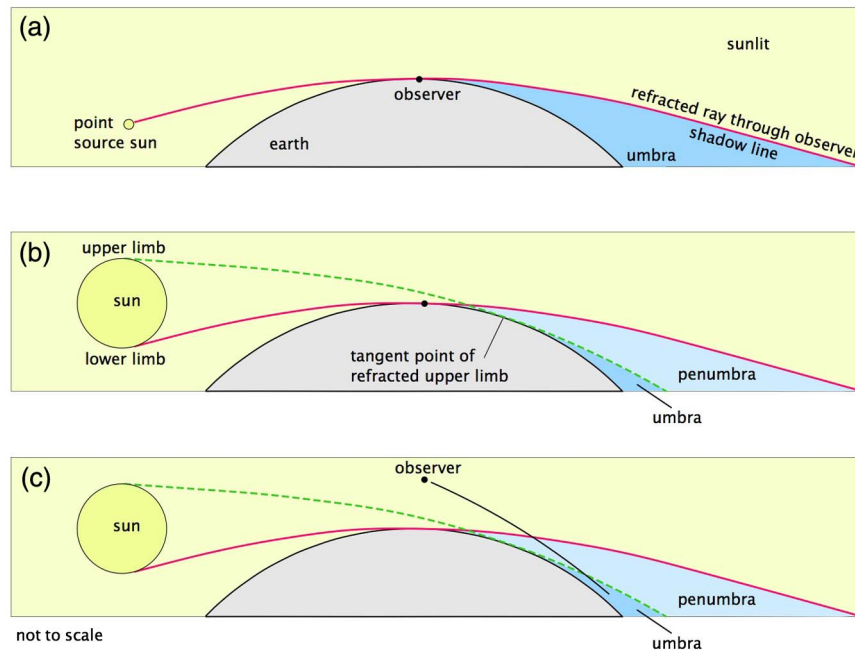
Fig. 19.   (a) Refracted shadow line for a point source Sun on the apparent horizon for an observer at sea level. (b) Refracted umbra and penumbra shadow lines for a 0.5° diameter Sun whose lower limb is on the refracted horizon as seen by a sea level observer. (c) Refracted umbra and penumbra shadow lines for a 0.5° diameter Sun whose lower limb is on the refracted horizon as seen by an elevated observer. An elevated observer can see into the umbra.

touching the horizon [Fig. 19(b)]. The ray from the lower limb is the same as the ray in Fig. 19(a). In this case, the shadow has two components, the umbra and penumbra. The ray from the upper limb is tangent to the Earth at a location that is hidden from the observer by the Earth. Here again, a sea level observer cannot see the shadow of the Earth.

If the observer is elevated by any significant amount, however, he can see the shadow, both umbra and penumbra [Fig. 19(c)]. The shadow will appear superimposed upon the lowest part of the dimmed horizon sky. It will also be below the geometrical horizon by an amount known to celestial navigators as "dip" [26].

If a sea level observer cannot see the shadow but still sees the dark segment, what is he seeing? We argue that he is seeing the dimmed atmosphere just above the horizon discussed by Lee [9] and clearly evident in Figs. 2, 3, 5, and 6. That it appears nearly the same color as the upper part of the BB makes the association with the Earth's shadow seem reasonable. As the upper part of the BB approaches the horizon, it slides into the HB and colors it blue. It is in the HB where Lee's horizon dimming takes place and the dimming is always present, regardless of the solar altitude, but passes unnoticed before sunrise. Thus the dark segment can have two components, depending on the observer's elevation: horizon dimming only for a sea level observer, and the shadow of the Earth for an elevated observer.

To validate the notion presented in Fig. 19(c), a ray trace of the atmosphere was performed for an observer at an elevation of 1 km and for a LOS altitude of −1° (Fig. 20). In this case, the shadow line is tangent to the Earth at the observer. The elevated observer's LOS passes into the shadow, something that cannot
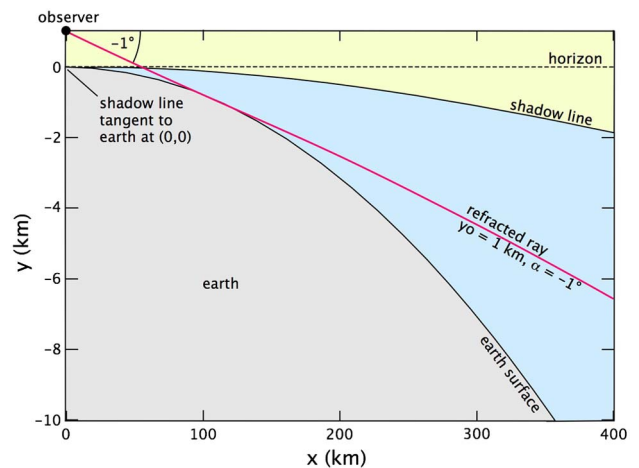
Fig. 20.   While an observer at the surface cannot see into the shadow, an elevated observer can. In this ray-traced diagram, the observer is at an elevation y_o of 1 km. While the ray trace is geometrically accurate, the large optical depth for such a low LOS prevents most of the light from the shadow from reaching the observer.

happen if the observer is on the surface, as Fig. 20 demonstrates. But as discussed in Section 7, optical depth limits how far the observer can see.

9. SUMMARY AND CONCLUSIONS

We have investigated the antisolar twilight based on new digital imagery, optical analyses, and ray tracing. Of particular importance

were the time-lapse videos and RGB analyses. Our findings have quantitatively confirmed many previous qualitative descriptions and extended the understanding of antitwilight. The rapid motion of the BV relative to the Sun's altitude is explained as a geometrical effect due to the small thickness of the atmosphere compared to the radius of the Earth. The dark segment is shown to be the normal dimming of the sunlit sky near the horizon and has only a component of the Earth shadow when the observer is elevated well above the surface of the Earth.

Four new terms are introduced in this paper: *horizon band, blue band, upper sky*, and *shadow line*. While we try to avoid using new terms, the first three are useful because they are based purely on observation (as opposed to being an interpretation like the term *shadow of the Earth*). Two of them (upper sky, horizon band) have received little recognition or attention, despite being physically identified with the optically thin and optically thick portions of the observer's LOS, respectively. The terms are consistent with previous terminology, but more importantly, they quantitatively unify the disparate terms used in the literature.

In a companion paper [27], the antitwilight was investigated theoretically using Monte Carlo techniques. The results are consistent with the findings of this paper and further enhance our understanding of the antitwilight.

APPENDIX A: OPTICAL DEPTH DETERMINATION

For the observations reported here, the broadband optical depth along the LOS for visible wavelengths was calculated from models used in the NASA/JPL Ephemeris Generator [28]. We used the NASA/JPL atmosphere (mid latitude summer) that included a typical aerosol load. From the ephemeris, the ratio of *magnitudes of extinction A* to *air mass X* is *k*:

$$k = A/X = 0.282 \text{ (units are airmass}^{-1}), \qquad \textbf{(A1)}$$

and is constant for all LOS altitudes for the observations reported here. Using the known relation [29]

$$A = 1.086\tau, \qquad \textbf{(A2)}$$

where τ is optical depth, we eliminate A between Eqs. (A1) and (A2) to get

$$\tau = 0.260X, \qquad \textbf{(A3)}$$

where k is the attenuation coefficient with units of (air mass)$^{-1}$. Setting $\tau = 1$ and solving for X, we find air mass $X = 3.85$. Using Rozenberg's [2] model for air mass,

$$X = (\cos z + 0.025e^{-11 \cos z})^{-1}, \qquad \textbf{(A4)}$$

where z is the zenith angle,

$$Z = 90° - a \qquad \textbf{(A5)}$$

where we find that $X = 3.85$ corresponds to $\alpha = 15°$ in the JPL ephemeris. Thus, for our observations, optical depth unity occurs about 15° above the horizon, and we have defined this altitude as the top of the horizon band (HB) for these observations.

The value of $k = 0.282$ is appropriate for clear skies in coastal southern California sea level observers. In contrast, for our observation at Oceano, California, on 31 December

2015, k was 0.116, much clearer than in Malibu. In this case, $\tau = 1$ occurs at $\alpha = 5.3°$. Thus, the altitude of the top of the HB depends on the clarity of the lower atmosphere.

A is a function of wavelength and varies considerably over the visible spectrum for pure Rayleigh scattering, being larger at shorter wavelengths. Effects from aerosols are much less sensitive to wavelength.

REFERENCES AND NOTES

1. G. V. Rozenberg, "Twilight phenomena, their nature, and use for atmospheric research," Sov. Phys. Usp. **6**, 198–249 (1963).
2. G. V. Rozenberg, *Twilight, A Study in Atmospheric Optics*, translated from the Russian by R. B. Rodman, ed. (Plenum, 1966).
3. M. Minnaert, *The Nature of Light and Colour in the Open Air*, translated by H. M. Kremer-Priest, revised by K. E. Brian Jay (Dover, 1954).
4. H. H. Neuberger, *Compendium of Meteorology*, M. Thomas, ed. (American Meteorological Society. Committee on the Compendium of Meteorology, 1951), pp. 61–78.
5. A. Meinel and M. Meinel, *Sunsets, Twilights and Evening Skies* (Cambridge University, 1983).
6. D. K. Lynch and W. Livingston, *Color and Light in Nature* (Cambridge University, 2001), Reprinted Thule Scientific (2010) http://www.colorandlightinnature.com.
7. T. F. Malone, *Compendium of Meteorology* (American Meteorological Society, 1951).
8. Glossary of Meteorology, American Meteorological Society (2000). Now available electronically at http://glossary.ametsoc.org/wiki/Main_Page.
9. R. L. Lee, Jr., "Horizon brightness revisited: measurements and a model of clear-sky radiances," Appl. Opt. **33**, 4620–4628 (1994).
10. R. L. Lee, Jr., "Twilight and daytime colors of the clear sky," Appl. Opt. **33**, 4629–4637 (1994).
11. R. L. Lee, Jr., "Measuring and modeling twilight's Belt of Venus," Appl. Opt. **54**, B194–B203 (2015).
12. R. L. Lee, Jr. and D. C. Mollner, "Tropospheric haze and colors of the clear twilight sky," Appl. Opt. **56**, G179–G187 (2017).
13. M. Annick, "Antitwilight Arch, Earth Science Picture of the Day," 23 November 2015 http://epod.usra.edu/blog/2015/11/antitwilight-arch.html.
14. J. V. Dave and C. L. Mateer, "The effect of stratospheric dust on the color of the twilight sky," J. Geophys. Res. **73**, 6897–6913 (1968).
15. J. A. Shaw, "What color is the night sky?" Opt. Photon. News **7**(11), 54–55 (1996).
16. J. A. Shaw, "The digital blue sky at night," Opt. Photon. News **16**(11), 18–23 (2005).
17. J. Dubois, "Contribution a l'étude de l'ombre de la terre," Ann. Geophys. **7**, 103–135 (1951).
18. E. O. Hulburt, "Explanation of the brightness and color of the sky, particularly the twilight sky," J. Opt. Soc. Am. **43**, 113–118 (1953).
19. We use the term "shadow line" in a specific sense, here defined as the ray that is tangent to the Earth and separates sunlit and shaded portions of the sky. At its tangent point, it defines the terminator of the Earth. This term shadow line is used to distinguish it from the frequently encountered term "twilight ray," which can refer to any ray involved with twilight formation that is not tangent to the Earth's surface.
20. J. M. Pernter and M. E. Felix, *Meteorologische Optik* (Wilhelm Braumüller, 1922).
21. Reported by Neuberger [4].
22. G. Boris, "Astronomical refraction in a polytropic atmosphere," Astron. J. **72**, 235–254 (1967).

23. G. G. Bennett, "The calculation of astronomical refraction in marine navigation," J. Navig. **35**, 255–259 (1982).

24. H. Neuberger, "Some remarks on the problem of the dark segment," Bull. Am. Meteor. Soc. **21**, 333–335 (1940).

25. The name "dark segment" (dark wedge) is used in various contexts to describe a dark region near the horizon before sunrise, and sometimes immediately after sunrise. It is often called the "shadow of the Earth," and before sunrise this is a correct if incomplete interpretation. In popular usage, the term "shadow of the Earth," however, refers only to the blue region, what we are calling the "blue band." As with the term "Belt of Venus," "Shadow of the Earth" has entered main stream usage, web searches finding "shadow of the Earth" over two hundred times more than "dark segment," and when correctly attributed to twilight phenomenology, much more because "dark segment" is frequently used to describe other things. We have chosen to avoid that term "shadow of the Earth" because it imparts an interpretation to the phenomena, and at this juncture we seek only to describe the effect. Furthermore, the horizon band (see Section 4, this paper), which has not been explicitly described before, is also part of the Earth shadow when the Sun is below the horizon, so assigning only the blue band to the Earth shadow is incomplete. Rather than settle on either "Shadow of the Earth" or "dark segment," we opted instead to explain the phenomena in terms of the observed structure of the anti-solar twilight and its dynamics as the solar altitude changes. All this being understood, we shall use the term "dark segment" to refer only to the dark band seen just above horizon immediately following sunrise and in the context of whether it is the shadow of the Earth or not.

26. N. Bowditch, *The American Practical Navigator* (National Imagery and Mapping Agency, 1802), US Navy (2002).

27. S. Richtsmeier, D. K. Lynch, and D. S. P. Dearborn, "Antitwilight II: Monte Carlo studies," Appl. Opt. **56**, G169–G178 (2017).

28. http://ssd.jpl.nasa.gov/horizons.cgi.

29. http://astrowww.phys.uvic.ca/~tatum/stellatm/atm5.pdf.phys.uvic.ca/~tatum/stellatm/atm5.pdf.